# Insights into Protein Kinase A Activation using cAMP Analogs and Amide H/$^{2}$H Exchange Mass Spectrometry

**TANUSHREE BISHNOI**

**NATIONAL UNIVERSITY OF SINGAPORE**

**2009**

# Insights into Protein Kinase A Activation using cAMP Analogs and Amide H/$^{2}$H Exchange Mass Spectrometry

**TANUSHREE BISHNOI**

**A THESIS SUBMITTED FOR THE DEGREE OF MASTER OF SCIENCE**

**DEPARTMENT OF BIOLOGICAL SCIENCES**

**NATIONAL UNIVERSITY OF SINGAPORE**

**2009**

# Acknowledgment

I gratefully thank my supervisor, assistant professor Ganesh S Anand for guiding me through the two-year journey of research and for giving me the opportunity to learn the Hydrogen/Deuterium Exchange Technique.

Special thanks to the Protein and Proteomics Centre, DBS, NUS for their continued cooperation in the use of the ABI 4800 MALDI-TOF/TOF Mass Spectrometer.

My sincere gratitude to the National University of Singapore Research Scholarship for funding my studies and stay.

I thank my friends Suguna, Petra, Moorthy, Venkat, Devang and Apoorva for always being there for me; Yungfeng for teaching me so much, in science and otherwise.

My deepest gratitude to my Guru H.H. Sri Sri Ravishankar and last but not the least to my family for always being my strength.

# Contents

## Summary

Cyclic adenosine 5'- monophosphate (cAMP) is an ancient signaling molecule and one of its primary eukaryotic targets is cAMP-dependent protein kinase A (PKA). PKA when inactive exists as a tetrameric complex of a dimeric regulatory subunit (PKA-R) and two monomeric catalytic subunits (PKA-C). The activity of PKA is regulated by binding of cAMP to the regulatory subunits in the inactive complex and releasing the PKA-C subunits. The signal for PKA-C dissociation and activation is hypothesized to be propagated through two charge relays, namely the Arg209- and Glu200- mediated signal relays, the molecular details of which are as yet unknown. This activation mechanism plays out through a ternary intermediate state consisting of the PKA-holoenzyme bound to cAMP, which occurs transiently before dissociation.The study of this transient complex can provide valuable insights into the activation mechanism of PKA and also help in the design of therapeutic moleclues. This intermediate state was studied using Rp-cAMPS, a cAMP analog which is capable of locking the ternary complex. Rp-cAMPS blocks the Arg209 mediated signal relay required for dissociation while the Glu200 mediated relay remains undisturbed. The ternary complex provided insights into the possible conformation of the intermediate state in PKA- activation as well as the role of the Glu200-mediated interaction. Amide Hydrogen/Deuterium exchange followed by mass spectrometry was employed to compare conformational differences of the holoenzyme in the free and the Rp-cAMPS bound form.

## List of Abbreviations

| | |
|---|---|
| Å | Angstrom |
| β-ME | β- Mercaptoethanol |
| DTT | Dithiothreitol |
| H | Hydrogen |
| $^{2}H$ | Deuterium |
| hr | hour |
| IPTG | Isopropyl β-D-thiogalactopyranoside |
| $K_d$ | Dissociation Constant |
| MALDI-TOF | Matrix Assisted Laser Desorption Ionization- Time of Flight |
| PBC | Phosphate Binding Cassette |
| mM | millimolar |
| mg | milligram |
| µg | microgram |
| min | minute |
| mL | millilitre |
| nM | nanomolar |
| µL | microlitre |
| SDS-PAGE | sodium dodecyl sulfate polyacrylamide gel electrophoresis |

## List of Figures

## List of Tables

# 1.Introduction

## 1.1 cAMP Signaling Pathway

Cyclic adenosine 5'- monophosphate (cAMP) acts as an important second messenger by mediating a plethora of cellular processes through the cAMP-mediated signaling pathway (Fig 1-1) (1,2). Extracellular ligands bind to a large family of integral membrane proteins called the G-protein-coupled receptors (GPCRs). Specific ligands bind to and activate each GPCR. This activation of the receptors is followed by a conformational change in the attached heterotrimeric G-protein complex which leads to the release of the Gs alpha subunit upon exchanging GDP for GTP. This activated Gs alpha protein then binds to a membrane bound enzyme called adenylyl cyclase and activates it. The activated adenylyl cyclase then catalyses the conversion of adenosine triphosphate (ATP) to cAMP (2).

cAMP translates the extracellular stimuli signals to downstream responses upon binding to specific receptors. The primary downstream receptor for cAMP in bacteria is the catabolite gene activator protein (CAP) which regulates gene expression (3). While in eukaryotic cells, cAMP binds to the regulatory subunit of cAMP-dependent protein kinase (PKA) (4,5) via a conserved cAMP binding motif. cAMP also binds the cyclic nucleotide-gated channels and the guanine nucleotide exchange proteins (EPAC) through the same motif (6,7,8). The levels of cAMP are regulated by phosphodiesterases (PDE) which hydrolyze cAMP into 5'-AMP.

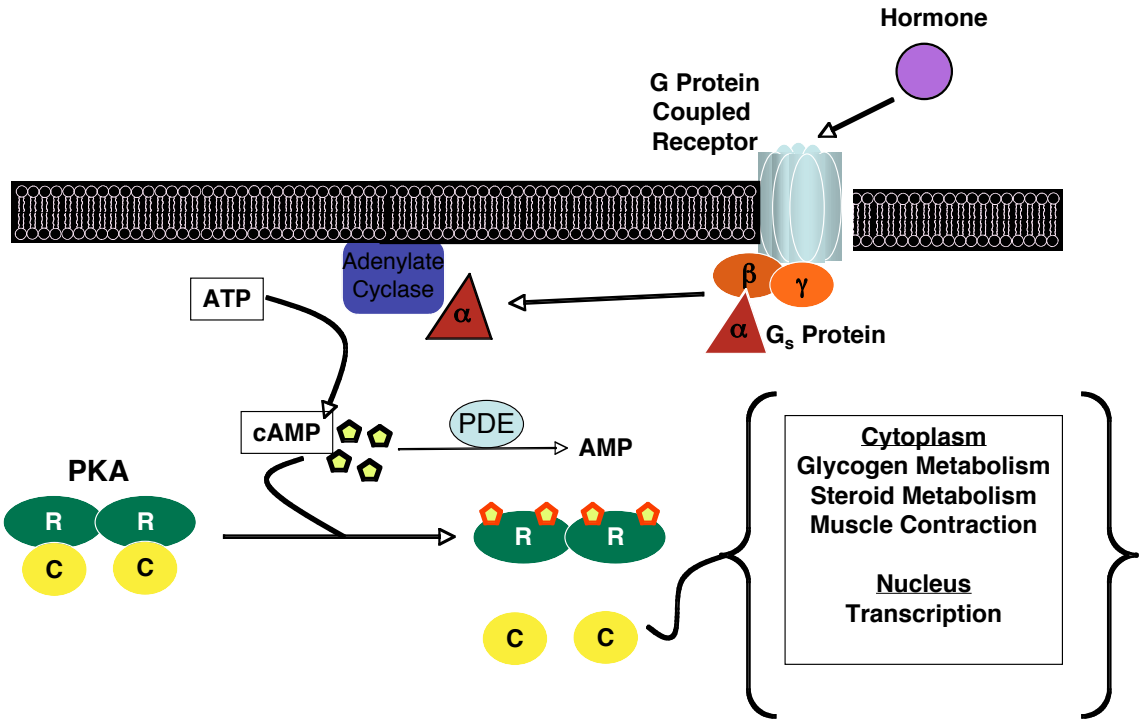


Figure 1-1. cAMP Signaling pathway (1,2)

### 1.2 cAMP-dependent Protein Kinase

Most known biological effects of cAMP in mammalian cells are mediated through the two ubiquitous isoforms of the regulatory (R) subunit of PKA, types I and II (9). The regulatory subunits of these isoforms are further classified into α- and β- forms each. The four distinct R-subunits (RIα, RIβ, RIIα and RII β) share a similar domain organization (Fig1-2) but are expressed by different genes (10). The amino terminal end consists of a docking/dimerization domain , which apart from allowing the R-subunits to exist as stable dimers also mediate docking to A kinase anchoring proteins(AKAPs). AKAPs act as scaffolds as well as help localize the holoenzyme to various cellular sites. A variable linker region follows which consists of a pseudosubstrate/inhibitor motif that interacts with the active site of the PKA catalytic subunit (PKA-C). Two tandem cyclic nucleotide binding

domains (CBD-A and CBD-B), at the carboxy terminal each have cAMP binding domains with distinct roles.

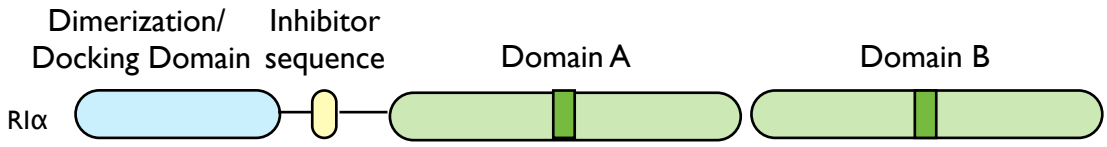


Figure 1-2. Domain organization of the PKA Regulatory subunit

The CBD-B acts as a doorkeeper by binding to a cAMP molecule and then allowing cAMP to access the CBD-A (11). The CBD-A has also been found to be part of the direct interaction site with PKA-C (12-14). The CBD-A has been shown to have a faster off-rate for cAMP compared to CBD-A (15). In the absence of cAMP, PKA exists as an inactive, tetrameric complex consisting of one PKA-R homo-dimer and two PKA-C monomeric subunits. The primary site of interaction between PKA-R and PKA-C is the Pseudosubstrate site which docks at the active site cleft of the kinase (Fig.1-5). While a peripheral site of intersubunit interactions distinct from the pseudosubstrate region, lies within the CBD-A.

The binding of cAMP to the holoenzyme is highly cooperative(16,17) where binding of the first molecule to the CBD-B domain leads to conformational changes in the A-domain allowing the second molecule of cAMP to access and bind the CBD-A, leading to dissociation of the holoenzyme complex. The inactivation of the enzyme follows the same mechanism with the C subunit binding the cAMP-bound R subunit and releasing one cAMP from the A domain first followed by release of the second cAMP from the B domain(18).

### 1.3 Physiological importance of RIα

The key compensatory role of RIα was discovered by gene knockout studies of R subunit isoforms in mice. In each case RIα was found to show compensatory regulation of PKA activity in tissues where the other R subunits are normally expressed. This unique regulatory role of RIα was further concretized by a knockout model of RIα in mice, which turned out to be embryonically lethal due to failed cardiac morphogenesis (19). This defect could however be rescued by a double knockout model of RIα and PKA-C, suggesting unregulated PKA-C activity was deleterious to the normal functioning of eukaryotic cells (19).

### 1.4 The four state model

There are two recognized stable conformations of the R subunit; the cAMP saturated, dissociated state and the holoenzyme state. However, two transient intermediate states must also be populated in traversing the shifts between the cAMP-bound and holoenzyme states (Fig 1-3). During activation, there must be a ternary complex of cAMP, PKA-R and PKA-C existing as a transient intermediate state prior to the dissociation of the complex. While, upon dissociation, the cAMP bound R subunit must pass through a cAMP-free and unbound to PKA-C state, before the reformation of the holoenzyme (20). The ternary intermediate state is relatively unstable compared to the R-C holoenzyme with a $K_D$ of 0.2μM (20,21).

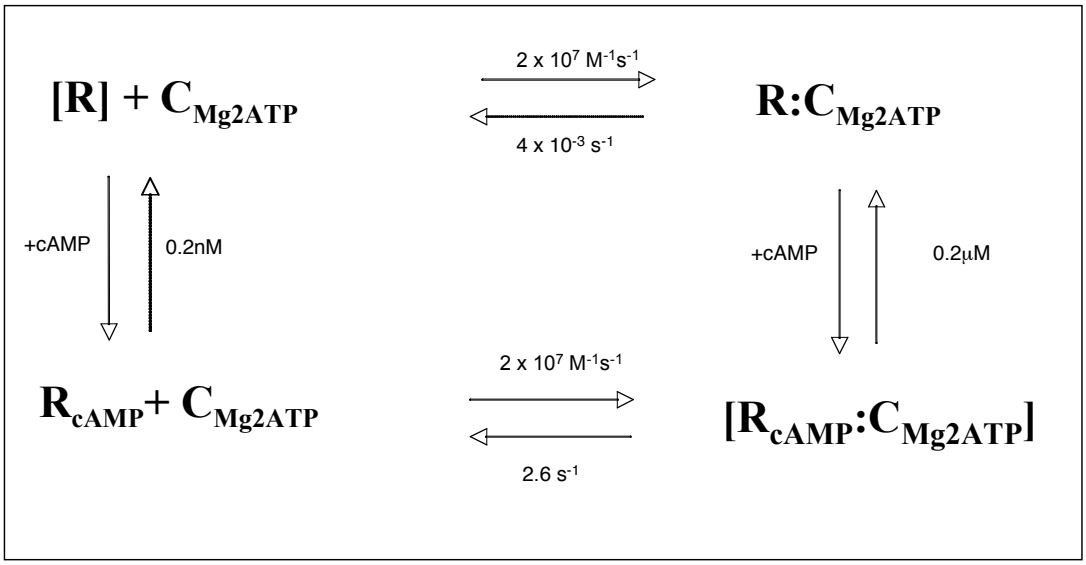


Figure 1-3. A proposed four state model for PKA activation based on the Kinetics of intersubunit interactions in the presence and absence of cAMP (20)

### 1.5 Deletion mutagenesis of RIα

Deletion mutants combined with yeast-two hybrid screens were used to study the distinct regions in CBD-A involved in mediating high-affinity interactions with PKA-C as well as for binding cAMP. The screens and further analysis identified RIα(94-169) as the minimum fragment required to inhibit PKA-C in a low micromolar range (22). While some residues in the C-helix(236-260) were identified as being important for high affinity binding to PKA-C as well as binding to cAMP. The estimated binding affinities of RIα(94-260) and RIα(94-244) were both found to be only marginally higher than the $K_D$ for full length RIα-C interactions (23). RIα(94-244) was hence highlighted as an ideal minimal model for binding and interaction studies of the RIα subunit with both cAMP and PKA-C (Fig.1-4).

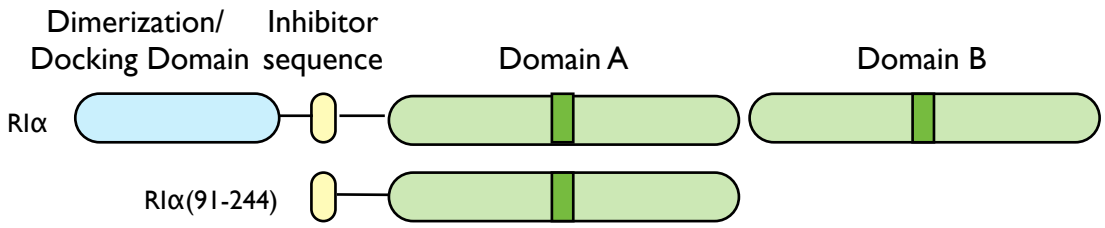


Figure 1-4. Domain Organization of RIα shows the boundaries of RIα(91-244). This is the minimal module that binds both cAMP and PKA-C with high affinity.

### 1.6 Kinetics of R subunit interactions with cAMP and C

The PKA-RC holoenzyme is a high affinity complex with $K_D$ values of 0.4nM and 0.2nM for the wild type RIα and the RIαΔ1-91 respectively (22). Although wild type PKA RIα in the absence of cAMP binds C-subunit with a faster association rate (1.0x $10^5 M^{-1}$ $s^{-1}$) than RIα(91-244)(2.3x $10^7$ $M^{-1}s^{-1}$) (20), the overall binding constants are very similar. The kinetics of interactions between the PKA-R and -C subunits have been studied in the presence of cAMP using stopped-flow fluorimetry with the deletion construct, RIα(91-244). The rates of dissociation of RIα from the C subunit were 700 fold faster ($K_D$ = 130nM) upon addition of cAMP while the association kinetics remained unchanged (20). The presence of substrates could also lead to dissociation of the complex but phosphorylated substrates release PKA-C faster, facilitating re-association of the holoenzyme complex (20).

### 1.7 Structural Insights into PKA RIα

As mentioned earlier, the RIα(91-244) double truncated mutant lacks the docking/dimerization domain as well as CBD-B and has been extensively studied by X-ray crystallography. Detailed analysis reveals that CBD-A in particular and both CBDs in general, consist of three α-helices and eight β-strands (24). The

helical regions make up the interface for PKA-C interactions while the β sheeted regions form the cAMP binding pocket (Fig.1-5).

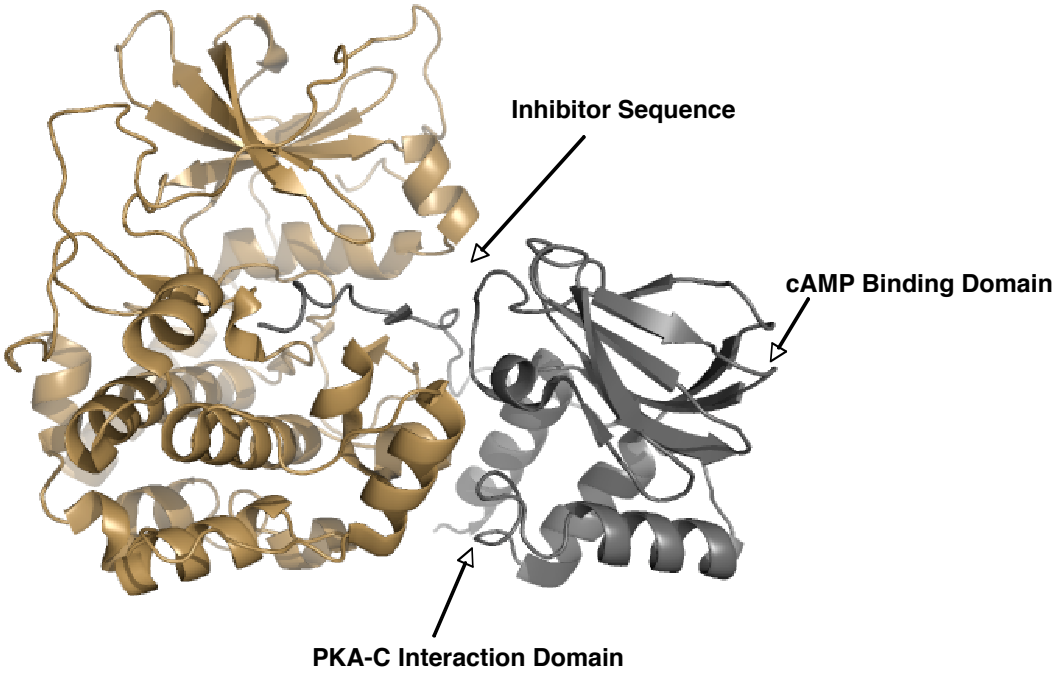


Figure 1-5. The RIα(91-244):C complex was drawn using Pymol with the pdb file (accession number- 1u7e) (27) where the sand colored region is PKA-C and the gray colored region is PKA RIα(91-244).

### *1.71 cAMP binding pocket*

The β-strands are arranged in two anti-parallel β sheets forming a β barrel subdomain. Each β-sheet consists of four strands connected in a jelly-roll topology (24). A pocket called the phosphate binding cassette (PBC), serves as the cAMP binding site and is highly conserved amongst the PKA-R family and cAMP-binding proteins in general (Fig.1-6) (25). cAMP binds both domains of PKA-R in a syn-conformation where the purine ring interacts primarily through

stacking interactions with a conserved aromatic amino acid at the C-terminal end of the C helix (Trp 260) (24).

The phosphate and the ribose ring form a network of hydrogen bonds as well as mediate electrostatic interactions with residues between β-strands 6 and 7. The 2'-OH of the ribose ring interacts with Glu200 electrostatically. Within the PBC, the equatorial exocyclic oxygen of the cAMP phosphate is anchored to Arg209 and Ala210 (Fig. 1-6).

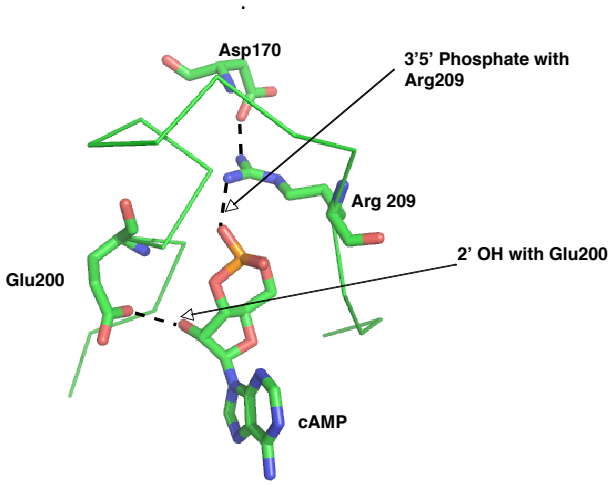


Figure 1-6. The Phosphate Binding Cassette(PBC) highlighting the Sites of Interaction with cAMP

Arg209 plays a very important structural role of a switch which connects binding of cAMP to the consequent release of PKA-C. It contacts the backbone carbonyl of Asn171 and the carboxylate of Asp170 to transmit the signal of cAMP binding (24). A signature sequence has been identified to be conserved within the PKA-R family. This sequence allows discrimination among PKA-R, cGMP-dependent protein kinase (PKG) and other cAMP binding regulators, as well as within identified PKA-R types and sub-types based on specific residues (25).

### *1.72 PKA-C binding region on RIα*

The PKA-C subunit docks at two loci on the R subunit, the pseudosubstrate region and the CBD-A. Within the CBD, previous studies using RIα(91-244) identified the C-terminal end of the A-helix (residues 144-148) as an important locus for intersubunit interactions (26).

### *1.73 Effects of PKA-C and cAMP binding on RIα(91-244)*

Solvent accessibility by amide $H/^{2}H$ exchange Mass Spectrometry studies showed that the cAMP-binding pocket (residues 202-221) is more exposed when the C-subunit is bound to it compared to the cAMP bound as well as the cAMP free forms (26). The region in the A-helix which shows protection from solvent upon binding the C subunit (residues 144-148), becomes more exposed upon cAMP binding as compared to the cAMP-free form.

### *1.74 Binding Surface on the Catalytic subunit*

RIα docks at three distinct surfaces on the C subunit.

*Site1* - The inhibitor sequence in the linker region of RIα docks at the active site cleft of the C-subunit. This sequence, Arg94-Arg-Gly-Ala/Ser-Ile98, has a phosphorylatable Ser or Thr in case of substrates and Ala or Gly in case of pseudosubstrates (PKA-RIα and PKI)

*Site 2* - The hydrophobic region of the PBC containing the Tyr205 interacts with a hydrophobic region on the G-helix of the C-subunit around the residue Tyr247.

*Site 3*- The residues Trp196 and Arg194 on the activation loop of PKA-C interact with Glu105 in the linker segment and Met 234 in the C-helix of RIα (27).

### *1.75 The cAMP switch / charge relay*

The equatorial exocyclic oxygen of the phosphate of cAMP forms a salt bridge with the guanidinium side chain of the invariant Arg209 in the PBC of RIα (91-244). The Arg209 contacts the side chain carboxylate group of Asp170 and transmits the signal of cAMP binding. This interaction also neutralizes the charge on Arg209. The signal is further relayed by Arg226 and Glu101 (hypothesized) leading to dissociation of PKA-C (Fig.1-7). This Arg residue is critical to this signal relay and replacing it with Lys abolishes high affinity cAMP binding at CBD-A (28).

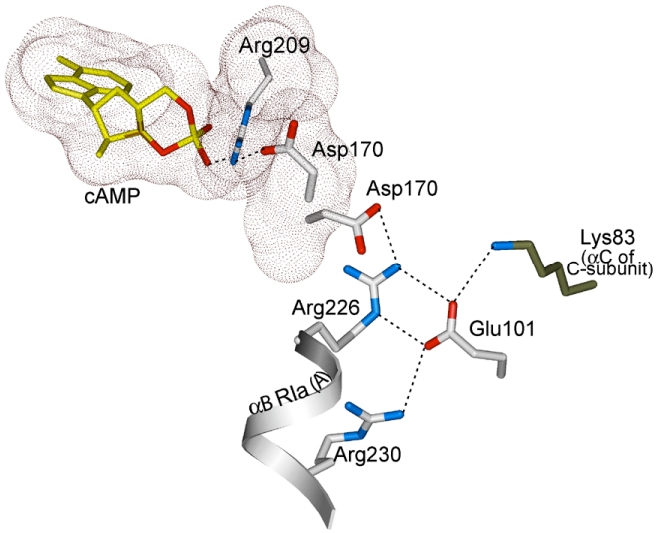


Figure 1-7. Hypothesized Charge Relay linking Arg209 with PKA-C dissociation

## 1.8 cAMP analogues

Cyclic nucleotide analogs present a huge potential for use in biochemical and pharmacological studies involving PKA. Several analogs have been synthesized and tested, however Rp-cAMPS (Rp-adenosine 3',5'-cyclic

monophosphorothioate) and related derivatives are the only known cAMP analogues that act as antagonists and competitive inhibitors of cAMP mediated PKA activation.

Rp-cAMPS has a single sulfur substitution of the exocyclic equatorial oxygen. The corresponding diastereomer Sp-cAMPS with a single sulfur substitution at the exocyclic axial oxygen is a cAMP agonist (Fig. 1-8). The sulfur substitution reduces the overall binding affinity for CBD-A by 400-fold for Rp-cAMPS and 5-fold for Sp-cAMPS (29). However, previous crystallographic studies revealed that the distance between the exocyclic equatorial sulfur of Rp-cAMPS to the NH1 atom of Arg209 was 2.6Å and between the equatorial oxygen of cAMP and the nitrogen atom was 3.1 Å (30). This suggested a stronger focal interaction between Rp-cAMPS and CBD-A despite a low overall affinity in comparison to cAMP.

The strength of this interaction has been attributed to formation of a stronger salt bridge-like electrostatic interaction between the surface charge of sulfur and the positively charged guanidinium side chain of Arg209. Resonance of electrons between the two exocyclic oxygens allows only weak hydrogen bonds to form between cAMP and the Arg209 side chain (30). This stronger interaction significantly weakens contacts between Arg209 and Asp170, resulting in termination of the signal for PKA-C dissociation, enabling Rp-cAMPS to lock the RIα(91-244)-C complex in the holoenzyme conformation rather than cAMP-bound conformation. However, the Rp-cAMPS analog allows the signal from the 2'OH- Glu200 interaction to remain undisturbed and hence the analog allows us to study the effects of this interaction on the ternary complex. On the other hand, Sp-cAMPS with a sulfur substitution in the axial exocyclic oxygen is a cAMP

agonist, causing the dissociation of the RC holoenzyme and hence acts as a close cAMP mimic.

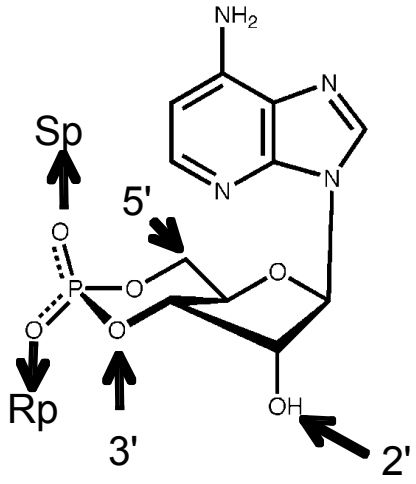


Figure 1-8. Diastereomeric Analogs of cAMP; Rp-cAMPS and Sp-cAMPS with a single sulfur substitution at the equatorial oxygen for Rp-cAMPS and at the axial position for the Sp-cAMPS*.*

# 2.Materials and Methods

## 2.1 Protein expression and purification

### *2.11 PKA RIα91-244 expression-*

The pRSET vector containing the RIα(91-244) gene insert was transformed into BL21DE3 cells and plated onto LB-Ampicillin agar plates. The transformants were then cultured overnight. This preinoculum was used to scale-up the culture to a 4 l culture volume. Cells were grown to an $OD_{600}$ of 0.8-1.0 at 37°C, with rotation at 220 rpm in an incubator shaker after which the cells were induced with 500mM IPTG and allowed to grow overnight (16-18 hr) at 22°C while rotating at 180 rpm. The cells were then centrifuged at 6000 rpm for 30 min at 4˚ C to pellet down the cells.

### *2.12 PKA RIα(91-244) purification-*

10 gm of the cell pellet was resuspended in lysis buffer A (20 mM MES, 100 mM NaCl, 2 mM EDTA, pH6.5), 5ml of the buffer A was used for every gram of cell pellet. The cell suspension was then sonicated to lyse the cells at 28% amplitude for 8 min at a 1-on,1-off pulse ratio. The cell lysate was then centrifuged at 13000 rpm for 30 min at 4°C to pellet the cellular debris. The supernatant was carefully separated into a new 50 ml tube.

The supernatant was then subjected to ammonium sulfate precipitation at 40% saturation for 1-2 hr at 4°C while being mixed with a magnetic stirrer. Salt was added gradually to prevent salting out of other proteins. The post-precipitation solution was then centrifuged at 4000 rpm for 10 min. The supernatant was discarded by aspiration or decantation. The pellet was resuspended in lysis buffer A. The suspension was incubated with activated and equilibrated cAMP-agarose resin overnight (12-16 hr). (method described below) At the end of the incubation period, the resin was separated from the suspension by centrifugation at 3000 rpm for 8 min at 4°C. The flow-through was carefully aspirated out and the resin was washed repetitively with the lysis buffer to remove nonspecifically bound proteins. Washes were carried out until no protein content was detected with Coomassie protein assay reagent.

The resin was then incubated with 10 ml elution buffer A (50 mM MES, 200 mM NaCl, 2 mM EDTA, 40 mM cGMP, pH 5.8) for 2-4 hrs at room temperature with constant agitation on a rocker. The elutions were collected by centrifugation of the resin at 3000 rpm for 8 min, at 4°C. The eluted protein was then concentrated using a Sartorius VIVASPIN 20 (10000 MWCO) filter device. The concentrated sample was subsequently loaded onto a GE HiLoad™ 16/60 Superdex™ 75 prep grade gel filtration column. The flow rate and fraction

volume were set at 0.5ml/min and 0.5ml respectively. The fractions corresponding to the resulting peak were collected (Fig.2-1).

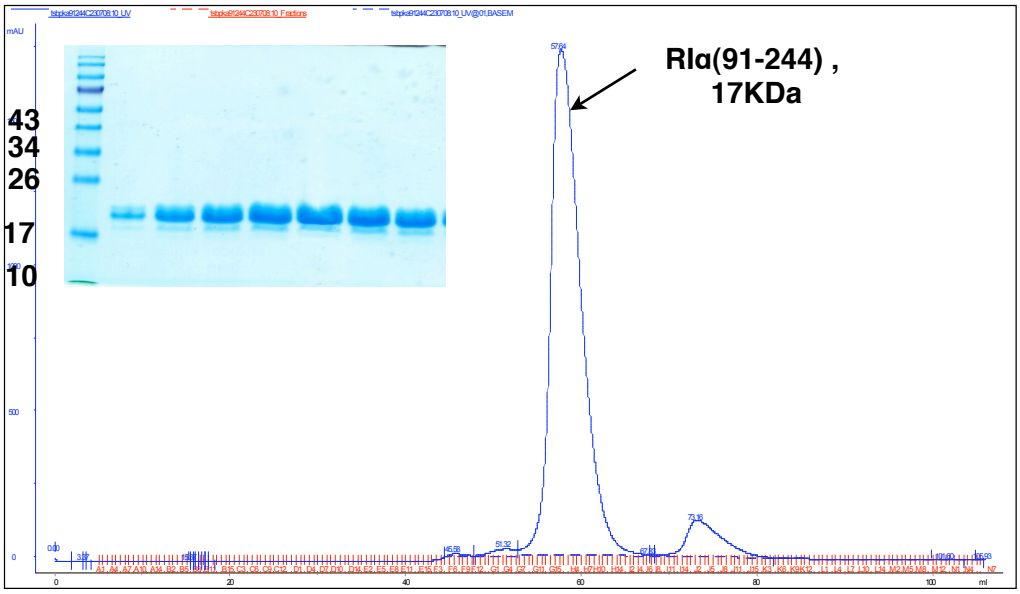


Figure 2-1. Gel-Filtration Profile for PKA RIα(91-244) with SDS-PAGE gel of purified sample(inlay). The marker label represents protein size in KDa.

### *2.13 Equilibration of cAMP agarose resin-*

NHS-activated Sepharose 4 fast flow (GE Healthcare), a pre-activated agarose matrix supplied by GE, was coupled with 8-AEA-cAMP through a spacer arm. A bed volume of 2 ml of the resin was taken in a 50 ml tube. The resin was reactivated by three alternative washes with High pH Buffer (200mM ethanolamine, 500 mM NaCl, pH 8.3) and Low pH Buffer (200mM potassium acetate, 500mM NaCl, pH 4.0). The activated resin was equilibrated by three-four washes with the lysis buffer. For every wash 30 ml of each buffer was added to the 50 ml tube containing the resin and centrifuged at 3000 rpm for 8 min at 4°C. Upon centrifugation, each buffer was carefully aspirated out while taking care not to disturb the resin bed.

### *2.14 PKA-C expression-*

The clone expressing N-terminal hexahistidine tagged PKA-C was transformed into BL-21DE3 cells and grown overnight in LB media with 100mM Ampicillin at 37° C with shaking at 220 rpm. The overnight culture was used as preinoculum for a large scale culture preparation (2l). The cells were grown to an $OD_{600}$- 0.8-1.0 and subsequently induced with 500mM IPTG. The culture was grown overnight (16-18 hrs) at 22°C, 180 rpm. The cells were then centrifuged at 6000 rpm for 30 min at 4°C. The cell pellet was stored at - 20°C.

### *2.15 PKA-C purification-*

1 gm of the pellet was weighed and resuspended in Lysis Buffer (20mM Tris, 300mM NaCl, 5mM β-ME, pH 7.5). The cell suspension was then subjected to sonication at 28% amplitude with a 1 sec-on, 1 sec-off pulse cycle for 5 min. The sonicated cell lysate was centrifuged for 30 min at 13000 rpm, 4°C, to pellet down the cellular debris. The supernatant was carefully aspirated and subsequently incubated with 0.5 ml of equilibrated TALON® Metal Affinity Resin. The incubation was carried out for 1-2 hrs at 4°C with constant rotation on a gyrating shaker. Subsequently the resin was washed with Lysis Buffer B. The protein was eluted out using elution buffer B (20mM Tris, 300mM NaCl, 200mM Imidazole, 5mM β-ME, pH 7.5). The eluted protein was then concentrated using Amicon-Ultra 15 (10000 MWCO) filter devices by centrifuging at 3000 rpm until the volume of the sample reduces to 2ml. The sample was then loaded onto a GE HiLoad™ 16 /60 Superdex™ 75 prep grade gel filtration column. The flow rate for the buffer (lysis buffer B) and the fraction volume settings were the same as used in PKA-R purification. Upon completion of the run, the fractions corresponding to the resulting peak were collected (Fig. 2-2).

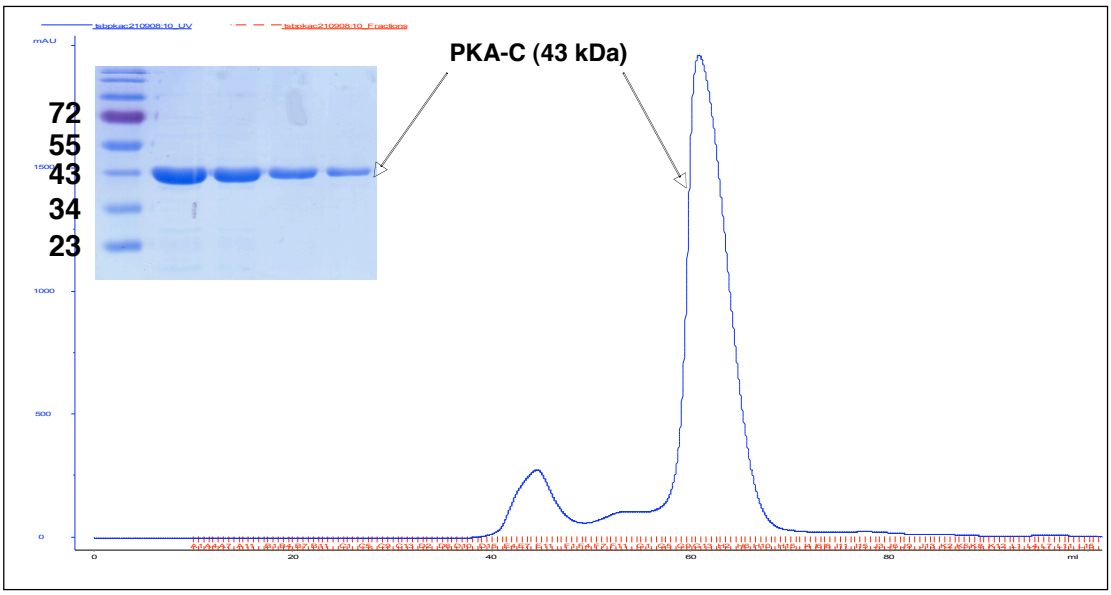


Figure 2-2. Gel Filtration profile of PKA-C with SDS-PAGE gel of purified sample (inlay).The first peak is aggregated PKA-C. The marker label represents protein size in KDa.

## 2.2 RIα(91-244):C holoenzyme formation

The concentrations of the RIα(91-244) and the PKA-C gel-purified samples were quantified using Coomassie protein assay reagent. The two proteins were then mixed in a molar ratio of 4: 1 (RIα(91-244):PKA-C) and dialyzed against 2l of MOPS holoenzyme buffer (50mM MOPS, 50mM NaCl, 2mM $MgCl_2$, 0.2mM ATP, 1mM β-ME, pH-7.0) for 16-18 hrs at 4°C. Upon completion of the dialysis, the sample was concentrated using Amicon Ultra-15 (10000 MWCO) filters. The concentrated sample was reloaded into the above mentioned gel-filtration column, with the flow rate and fraction volume set at 0.2 ml/min and 0.5 ml respectively. The resulting profile showed two peaks, the first higher molecular weight peak corresponded to the RIα(91-244):C holoenzyme while the second peak corresponded to the excess unbound RIα(91-244). The holoenzyme peak fractions were collected and concentrated to 6 mg/ml (Fig.2-3).

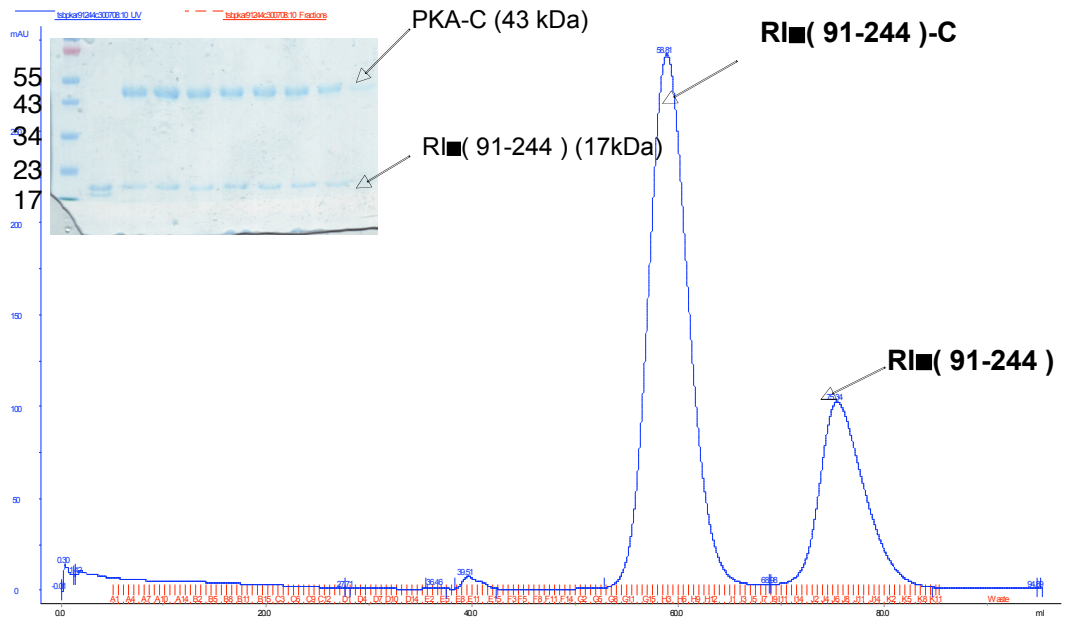


Figure 2-3. Gel (Sepharose) Filtration profile of RIα(91-244):C holoenzyme formation, with the first peak representing the complex and the second peak representing excess RIα(91-244) . Inlaid is the SDS-PAGE gel of the first peak. Comparison of the elution profile with standards provided by the manufacturer showed that RIa(91-244) eluting as a monomer (data not shown- http://www.gelifesciences.com/aptrix/upp01077.nsf/Content/Products?OpenDocument&moduleid=165424). Independent tests by several groups including our own showed that the RIα(91-244):C and RIα(91-244) prepared in exactly the same manner described above generated monomeric forms of the holoenzyme complex (Kim et al. (2005), reference) and RIα(91-244) (Badireddy, 2010, Manuscript submitted).

### *2.21 Rp-cAMPS bound RIα(91-244)-C-*

The cAMP analog, Rp-cAMPS was added to a final concentration of 1mM to 50 µl of the RC sample.

### *2.22 Sp-cAMPS bound RIα(91-244):C-*

Sp-cAMPS is a cAMP analog and addition of the same to the RIα (91-244):C complex leads to dissociation. Hence an experiment was designed by using information about the kinetics of the RIα(91-244):C complex in the presence of Sp-cAMPS. In this experiment, increasing relative concentrations of one interacting partner versus the other, from the values of the $K_{D,}$ ensures

nearly all of the other partner to be in the complexed form (Anand, Bishnoi,Taylor and Johnson (2009) (Manuscript in preparation)). The program “% Bound” was used to calculate the above mentioned concentrations (31). Final concentration 30 μM PKA-C and 10 μM RIα(91-244) were mixed with 10 μM Sp-cAMPS to form the ternary complex.

### 2.3 Amide Hydrogen/Deuterium Exchange

Amide hydrogen/deuterium exchange followed by mass spectrometry is a method used to analyze the structure and dynamics of proteins. Some hydrogen atoms in proteins are capable of exchanging with the hydrogen atoms of the surrounding solvent molecules. If deuterium oxide is used as a solvent then the isotope of hydrogen, deuterium gets incorporated into the protein and as deuterium is one mass unit heavier than hydrogen so upon deuteration the protein also becomes correspondingly heavy and this change in mass can be monitored by high resolution mass spectrometers.

Amongst the three kinds of hydrogens in proteins, hydrogens covalently bound to carbon atoms, side chain hydrogens and backbone amide hydrogens, only the backbone amide hydrogens exchange at a rate that can be detected. Since backbone amide hydrogens are involved in hydrogen bond formation in secondary structure elements, their exchange rates are reflective of structural stability. Also studying exchange rates of backbone amide hydrogens present at the surface of proteins can be used to detect binding of other proteins and analyze protein complexes.

This exchange rate is specific and is determined by the protein structure and solvent accessibility and is also strongly pH dependent.

Exchange reactions are carried out at physiological pH(7.0-8.0) since proteins are closest to their native conformational state in this range and since the exchange rate for backbone amide hydrogens is minimum at pH 2.6 , so by rapidly lowering the pH the exchange reaction can be slowed down or quenched. Upon quenching the exchange reaction, the protein is digested by a protease in order to localize and quantify the deuterium exchange. Pepsin, an acid protease which is active at low temperature is mostly used, it maintains the quench pH which ensures minimum back exchange. Other acid stable proteases can also be used to achieve different sequence coverage and resolution.

The exchange experiment was carried out by incubating 2 µl of the protein with 18 µl deuterated MOPS buffer for 0,0.5,1,2,5,10 min time points at room temperature. The amide exchange was terminated by adding 180 µl of the quench buffer (0.05% TFA, chilled). Peptic digestion was carried out by adding 100 µl of the quenched sample to 50 µl of activated pepsin slurry. The digestion was carried out on ice for 5 min with periodic vortexing every 30 sec.

The digested sample was then centrifuged at 13900 rpm for 15 sec to pellet the pepsin slurry and the supernatant was aspirated out into three 18 µl aliquots and immediately flash frozen in liquid nitrogen. The frozen samples were stored at -70°C till data collection (32).

**2.4 Data collection-**

The samples were transferred to a liquid Nitrogen can and taken to the Mass Spectrometry facility. Each sample is quickly thawed and 2µl of the sample is mixed with 2 µl of matrix (3mg α-Cyano-4-hydroxycinnamic acid (Sigma)) dissolved in 200 µl Acetonitrile, 200 µl Ethanol and 200 µl 0.1% TFA (pH 2.5). 0.5 µl of this mixture was spotted onto a MALDI-TOF plate. The data was

collected from the spot using the ABI 4800 MALDI-TOF/TOF Mass Spectrometer (33).

**2.5 Data Analysis-**

Each sample when injected into the ABI 4800 MALDI-TOF/TOF Mass Spectrometer yielded a range of spectra. Spectra were calibrated using Data Explorer (Applied Biosystems) with internal peptide masses- 1011.4609 (RIα (91-244), residues 222-229) and 1793.9704 (C-subunit, residues 247-261), pepsin proteolytic fragments. The centroid of the peptide envelopes were measured using Decapp Mass Spec Isotope Analyzer computer program (32). The calibrated peptides were then centroided using program “Decapp”. The program calculates the centroid of each peak spectrum by averaging the intensity of the constitutive peaks. The centroids for the undeuterated sample (proteo) were also calculated. The side chain correction value for each peptide was determined by adding the number of exchangeable side chain amide hydrogens and multiplying that value to a dilution factor of 0.045. This factor was calculated considering the various steps of dilution undergone by the sample, i.e. ten times dilution upon mixing with deuterated buffer (90% diluted), followed by ten times dilution by the quench buffer (9%diluted) and finally two times dilution by mixing with Matrix (4.5% dilution). The back-exchange factor was calculated to be ~66%, so all centroid values were multiplied by a back exchange factor or 3.0 to calculate the experimental deuterium exchange levels. The experimental number of exchanged deuterons for each peptide was calculated by subtracting the undeuterated centroid value and the side-chain correction value from the centroid value and dividing it by the back exchange factor. This value indicates the average number of deuterons exchanged.

# 3. Results

## 3.1 Measurement of solvent accessibility changes in the holoenzyme of PKA upon binding of Rp-cAMPS

In order to investigate the basis for the antagonist effects of Rp-cAMPS on PKA activation, we set out to compare the solvent accessibility changes between the free and Rp-cAMPS-bound states of PKA holoenzyme. Solvent accessibility measurements were made by amide H/$^2$H exchange MALDI-TOF mass spectrometry (32). The two samples chosen for a comparative analysis were the PKA holoenzyme formed between the C-subunit and a deletion fragment of RIα, RIα(91-244) in the absence and presence of Rp-cAMPS.

RIα(91-244) is the smallest deletion fragment of PKA RIα that binds the C-subunit with an almost similar affinity as full-length RIα (20), (22). In addition to binding the C-subunit with high affinity, this fragment has additional advantages. It is monomeric and contains a single cAMP binding site making it a facile model to understand detailed and structure and dynamics of intersubunit interactions in PKA by both X-ray crystallography (27) and NMR (34). These reasons were the basis for our choice of this deletion fragment complex to study the effects of Rp-cAMPS binding by Amide H/$^2$H exchange coupled to MALDI-TOF mass spectrometry. Furthermore, this technique is better suited to analyze smaller proteins due to better protein sequence coverage as a result of the lower likelihood of overlapping pepsin-digest fragments (32).

Deuterium incorporation into the rapidly exchanging backbone amides in the RIα(91-244):C complex in the free and Rp-cAMPS bound states were carried out by incubation of all protein samples in MOPS buffer in $D_2O$ at 25° C. Reactions were quenched by lowering temperature and pH to 2.5 as described in

materials and methods. Pepsin cleavage under quench conditions allowed localization of the observed changes in solvent accessibility to specific pepsin proteolytic peptide fragments as described previously (24). A total of 8 peptides from RIα(91-244) and 15 peptides from the C-subunit were analyzed. Tables 1 and 2 summarize the extent of deuteration of all peptides from RIα(91-244) and the C-subunit respectively. For select segments of both subunits where changes were observed, plots of the time-course of deuteration are also shown (Fig.3-1,3-2,3-3). Average number of deuterons exchanged during a 10-min exposure to deuterium oxide were determined from fitting plots of the time course of deuteration to a single-exponential equation and reported from replicate experimental measurements and standard error of the fits to the amplitude term of a single-exponential equation. This method of data presentation has been demonstrated to result in the same conclusion as with average numbers of deuterons incorporated after 10-min deuterium exchange from three independent experiments (26). To distinguish between specific and non-specific effects of the binding of Rp-cAMPS to PKA, we set out to use Sp-cAMPS as a control in our solvent accessibility measurements. Due to the much lower affinity of the R and C-subunits in the presence of Sp-cAMPS compared to the Rp-cAMPS, the concentrations of the R and C-subunits used in the experiment were modified for the Sp-cAMPS binding experiments to ensure saturation of the complex in the presence of Sp-cAMPS. Two experimental conditions were attempted. In order to measure solvent accessibility changes within RIα(91-244) in the presence of Sp-cAMPS and C-subunit, an excess of the free C-subunit was used and similarly an excess of RIα(91-244) was used to maintain all of the C-subunit in an R-subunit-bound state in the presence of Sp-cAMPS. The presence of an excess of one subunit relative to the other in each

of these experiments decreased the overall signal and only a few peptides could be analyzed compared to the holoenzyme in the presence of Sp-cAMPS. Overall, a majority of the peptides analyzed showed increased solvent accessibility upon binding Rp-cAMPS. Peptides from each of the two subunits have been separated and grouped on the basis of their primary sequences.

### *3.11 Solvent accessibility changes in the RIα (91-244) :C complex when bound to Rp-cAMPS*

#### *3.111 The α-Xn helix*

The α-Xn helix represented by two peptides (m/z = 1783, residues 111-125, m/z= 1619, residues 122-136) showed increased solvent accessibility of 17.8% and 14.5% respectively upon binding Rp-cAMPS. Peptide spanning residues 111-125 in the sample of PKA with Rp-cAMPS showed nearly maximum deuteration within 10-min suggesting this is part of a highly dynamic region connecting the pseudosubstrate region with the cAMP:A domain (Fig. 3-1).

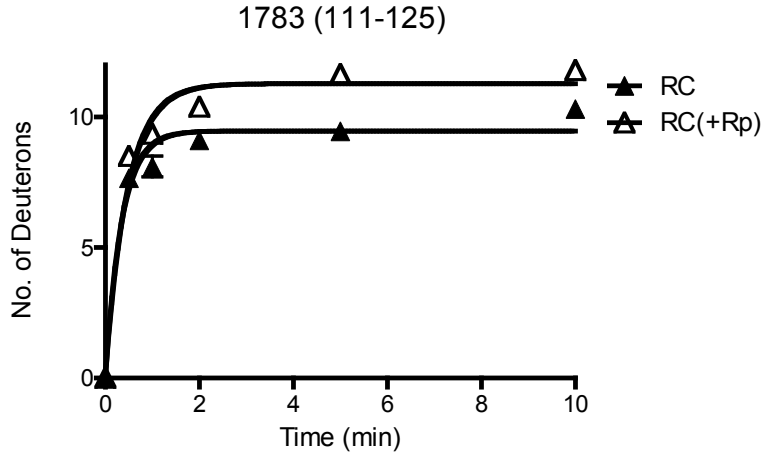


Figure 3-1. Time-course plot for deuteration of the RIα(91-244) α-Xn helix peptide (111-125)

### *3.112 The loop connecting α:Xn to α:A and 1st turn of α:A helix*

The A-helix peptide m/z = 976.4, residues 136-143, which is one of the regions that form part of the extensive C-R intersubunit interface based on the X-ray crystal structure of the PKA holoenzyme (27) and contains a few residues such as His 136 and Glu 143 which mediate salt bridges with residues in the C-subunit, was deuterated to the same extent in the bound form.

### *3.113 The Phosphate-binding cassette (PBC)*

One peptide (m/z = 1931.15, 204-221) spanned a large part of the phosphate-binding cassette (PBC), composed of β-strand 6, a short P-helix, a loop, and β-strand 7. Consistent with the fact that this is the cAMP-binding site, the solvent accessibility was lower in the Rp-cAMPS-bound samples reflective of occupancy of this site. (Fig. 3-2). This region is highly shielded from solvent as a large proportion of the residues in this peptide do not exchange within 10 min, indicating that this region is largely solvent inaccessible (26).

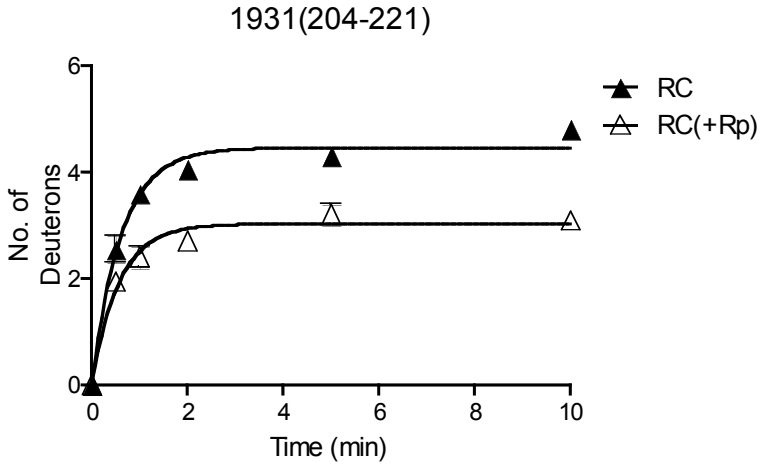


Figure 3-2. Time-course plot for deuteration of the RIα(91-244) peptide covering the PBC

### *3.114 α:B-helix (residues 222-229) and α:C (residues 230-244)*

A bulk of the peripheral intersubunit interface in the RIα(91-244):C complex is contributed by residues from the α:B and adjoining residues from the α:C helix. Interestingly a bulk of this region did not show any differences in solvent accessibility upon binding of Rp-cAMPS. Three peptides, m/z = 1011.46, residues 222-229, m/z = 1046, residues 230-238 (Fig.3-3) and m/z = 881.51, residues 239-244 showed no difference in solvent accessibility while one overlapping peptide, m/z=994.50, residues 238-244 showed increased solvent accessibility (Fig.3-3) (increased deuteration by 1) upon binding Rp-cAMPS. By subtractive analysis, the site of increased exchange can be localized to the backbone amide of residue Arg 239 and its environment. This is consistent with the predicted role of this residue in mediating contacts with the 2'OH moiety of cAMP via Glu 200 of the PBC on the basis of molecular dynamics simulation experiments (33).

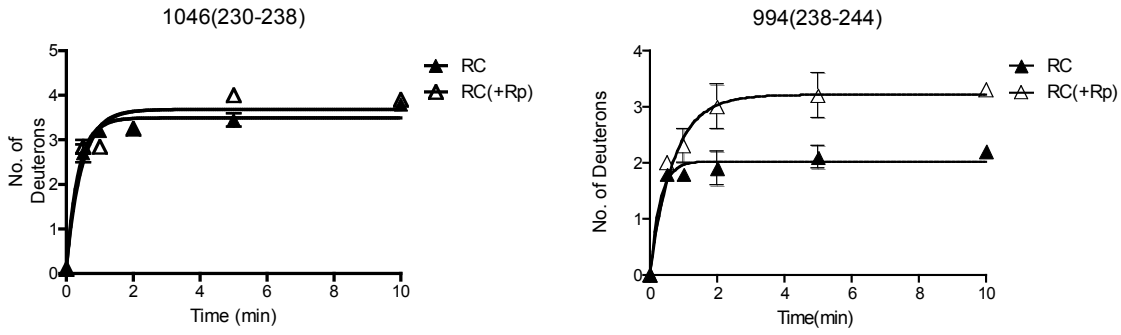


Figure 3-3. Time-course plot for deuteration of the two RIα(91-244) C-helix peptides, (230-238) and (238-244).

### *3.115 Catalytic subunit*

The N-terminal lobe of the C-subunit showed no difference between the antagonist bound and free forms for all regions except for the peptide, m/z =1530, residues 28-40 which shows greater exchange in the former state.

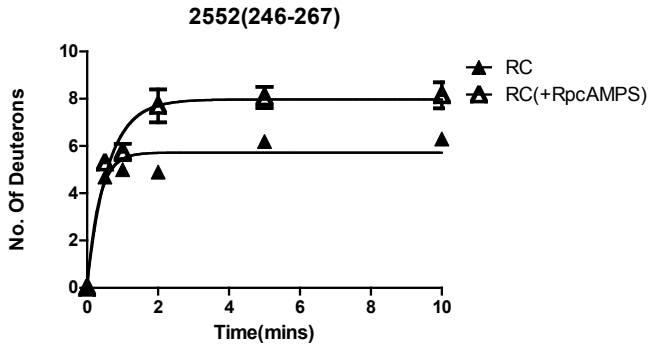


Figure 3-4. Time-course plot for deuteration of the PKA-C peptide (246-267)

The C-terminal lobe on the other hand was found to have increased solvent accessibility upon Rp-cAMPS binding to the RIα(91-244):C.

This was shown by peptides m/z = 1708, residues 237-250, m/z = 2552, residues 246-267 (Fig. 3-4), m/z = 1347, residues 278-289, m/z = 303-327, residues 303-327.

## 3.12 Solvent accessibility changes in the RIα(91-244) subunit when bound to Rp-cAMPS

The RIα(91-244) truncated regulatory subunit was then looked at in apo form and compared with the Rp-cAMPS analog. The α-Xn helix and B helix peptides, m/z=1783, residues 111-125, m/z=1011, residues 222-229 respectively showed no difference in solvent accessibility. The C-helix peptide m/z= 881, residues 239-244 which lies at the end of this truncated protein shows the same solvent exposure upon binding the ligand, whereas the peptide m/z=1046,

residues 230-238 in the same helix showed an increase in one deuteron upon binding. The phosphate binding cassette showed a protection of 3 deuterons between the unbound and Rp-cAMPS bound form which is about 18% less deuteration (Table 1).

**Table 1 - Maximum H/$^2$H Amide Exchange of the Regulatory Subunit (RIα (91-244) ) Complexed to PKA-C**

| Fragment of RIα-subunit (m/z) | No. of amides | RIα (91-244):C (apo) | RIα (91-244):C (+Rp-analog) | RIα (91-244) (apo) | RIα (91-244) (+Rp-analog) |
|---|---|---|---|---|---|
| α:Xn | | | Dex* | | |
| 111-125 (1783) | 13 | 9.6±0.3 | 11.3±0.3* | 12.4±0.1 | 12.7± 0.2 |
| 122-136 (1619) | 14 | 8.3±0.2 | 9.5±0.3* | ND | ND |
| A-helix | | | | | |
| 136-143 (976) | 7 | 3.7±0.2 | 3.2±0.2 | ND | ND |
| Phosphate -binding cassette | | | | | |
| 204-221 (1931) | 16 | 4.5±0.1 | 3.1±0.1* | 6.3±0.4 | 3.5±0.1 |
| C-helix | | | | | |
| 222-229 (1011) | 7 | 1.1±0.1 | 1.0±0.2 | 1.5±0.2 | 1.6±0.4 |
| 230-238 (1046) | 8 | 3.5±0.1 | 3.7±0.2 | 5.4±0.4 | 6.4±0.9 |
| 238-244 (994) | 6 | 2.0±0.1 | 3.2±0.2* | ND | ND |
| 239-244 (881) | 5 | 2.3±0.1 | 2.3±0.1 | 2.9±0.4 | 2.9±0.2 |

* No. of deuterons exchanged over a 10 min time course obtained from kinetic plots of deuterons which fits best to a single exponential model. This model approximates the rates of fast changing deuterons (mainly solvent accessible amides) to a single rate.
ND - not detected.

**Table 2 - Maximum H/$^2$H Amide Exchange of the Catalytic Subunit Complexed to RIα(91-244)**

| Fragment of C-subunit (m/z) | No. of amides | RIα(91-244):C (apo) | RIα(91-244):C (+Rp-cAMPS) |
|---|---|---|---|
| | | Dex* | |
| 18-26(1068) | 8 | 5.9±0.1 | 6.4±0.2 |
| 28-40(1530) | 11 | 9.0±0.2 | 9.8±0.3* |
| 41-54(1584) | 13 | 6.2±0.2 | 5.8±0.3 |
| 44-54(1194) | 10 | 3.6±0.2 | 4.0±0.2 |
| 92-100(1088) | 8 | 2.7±0.1 | 2.9±0.1 |
| 133-145(1628) | 11 | 2.8±0.2 | 3.2±0.1 |
| 163-174(1486) | 10 | 2.0±0.2 | 1.9±0.1 |
| 164-174(1373) | 9 | 1.0±0.2 | 0.9±0.1 |
| 212-221(1167) | 9 | 3.0±0.1 | 3.7±0.1* |
| 237-250(1708) | 11 | 2.0±0.1 | 2.7±0.1* |
| 246-267(2552) | 20 | 5.7±0.4 | 8.0±0.3* |
| 247-261(1793) | 13 | 5.3±0.2 | 6.3±0.2* |
| 247-264(2083) | 16 | 7.4±0.3 | 7.8±0.3 |
| 247-267(2439) | 17 | 5.5±0.2 | 6.1±0.2 |
| 278-289(1347) | 11 | 2.5±0.1 | 3.9±0.1* |
| 306-326(2379) | 17 | 9.6±0.2 | 10.1±0.3 |
| 303-326(2676) | 20 | 11.1±0.2 | 12.3±0.3 |
| 303-327(2823) | 21 | 11.5±0.8 | 13.4±0.4* |
| 305-326(2492) | 18 | 10.6±0.1 | 11.8±0.3* |

* No. of deuterons exchanged over a 10 min time course obtained from kinetic plots of deuterons which fits best to a single exponential model. This models approximates the rates of fast changing deuterons(mainly solvent accessible amides) to a single rate.

## 3.2 Solvent accessibility changes in the RIα(91-244):C complex when bound to Sp-cAMPS

The ternary complex of RIα(91-244):C with Sp-cAMPS presented limited coverage owing to the design of the experiment and the nature of the analog. The A-helix covered by the peptide m/z= 1594, residues 136-148 showed increased exchange of five deuterons upon binding Sp-cAMPS (Fig. 3-5). While the C-helix peptide m/z =1046, residues 230-238 showed protection from solvent in the ternary complex as compared to the holoenzyme (Fig. 3-5). The C-terminal of the C-helix however showed no change upon binding Sp-cAMPS; this region was covered by the peptide m/z= 994, residues 238-244.

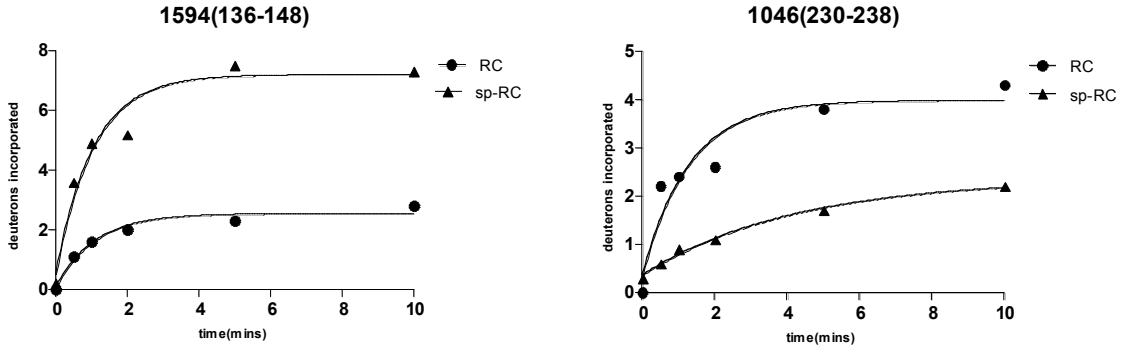


Figure 3-5. Time-course plot for deuteration of the A-helix peptide (136-148) and the C-helix peptide (230-238)

## 3.3 Solvent accessibility changes in the RIα(FL):C complex when bound to Rp-cAMPS

### *3.31 RIαFL- A domain*

The peptides, m/z = 1783, residues 111-125 and m/z = 1594, residues 136-148 which belong to the α-Xn helix and the A-helix respectively showed no change in solvent accessibility for the complex. As expected, the phosphate binding cassette showed increased protection from solvent upon binding with the Rp-analog, as shown in the peptide, m/z = 2115, residues 201-220. The C-helix peptides m/z = 1011, residues 222-229, m/z = 933, residues 230-247, m/z = 1286, residues 239-247 showed no change in deuteration after incorporation of the Rp-cAMPS (Table 3).

### *3.32 RIαFL- B domain*

The peptides which span the cAMP binding domain B showed no change in deuterium incorporation upon binding to the cAMP antagonist with the exception of peptides m/z = 1175, residues 355-363 and m/z = 1523, residues 363-374 showed increased deuterium incorporation (Table 3).

## 3.4 Solvent accessibility changes in the RIαFL subunit when bound to cAMP and Rp-cAMPS

### *3.41 RIαFL- A domain*

The full length R subunit free of cAMP was compared with cAMP and Rp-cAMPS bound forms. The A-helix peptide m/z = 1594, residues 136-148 showed no change between the cAMP bound and free forms but showed increased solvent accessibility upon binding the Rp-analog. The phosphate binding cassette which was covered by the peptide, m/z = 2115, residues 201-220 more protection in the Rp-bound form as compared to the c-AMP bound form. The N-terminal of the C-helix covered by the peptides m/z = 1011, residues 222-229 and m/z = 933, residues 230-247 showed increased solvent accessibility upon

binding Rp-cAMPS compared to the cAMP bound protein. This trend was reversed in the C-terminal peptide m/z = 1286, residues 239-247 where ligand binding led to more protection progressively from cAMP to Rp-cAMPS (Table 3).

### *3.42 RIαFL- B domain*

The N-terminal peptides m/z = 1561, residues 255-267, m/z = 1330, residues 299-309, and m/z = 1338, residues 310-321 showed no significant change in protection between the three states. The three peptides m/z = 1953, residues 337-353, m/z = 1175, residues 355-363 and m/z = 1523, residues 363-374 showed reduced solvent accessibility in the Rp-cAMPS bound state as compared to the cAMP bound state. The free state was found to be more accessible than the ligand bound states (Table 3).

**Table 3- Maximum H/$^2$H Amide Exchange of the RIα FL complexed with the Catalytic subunit**

| Fragment of RIα-subunit (m/z) | No. of amides | RIαFL:C (apo) | RIαFL:C (+Rpanalog) | RIαFL (apo) | RIαFL (+Rpanalog) |
|---|---|---|---|---|---|
| cAMP: A domain | | | Dex* | | |
| α:Xn 111-125 (1783) | 13 | 11.2±0.4 | 11.6±0.3 | 10.4±0.2 | 9.7±0.5 |
| A-helix 136-148(1594) | 12 | 3.1±0.4 | 3.5±0.5 | 4.3±0.1 | 5.9±0.5 |
| Phosphate -binding cassette 204-221 (1931) | 16 | 5.8 | 2.4±0.1 | 4.5±0.2 | ND |
| C-helix 222-229 (1011) | 7 | 0.9±0.1 | 1.7±0.3 | 1.5±0.2 | 1.9±0.2 |

| | | | | | |
|---|---|---|---|---|---|
| 230-237 (933) | 7 | 1.2±0.1 | 1.2±0.1 | 2.5±0.3 | 3.4±0.1 |
| 239-247 (1286) | 8 | 1.4±0.1 | 4.9±0.6 | 4.5±0.3 | 2.1±0.3 |
| cAMP: B domain | | | | | |
| 255-267(1561) | 12 | 5.2±0.1 | 5.1±0.1 | 5.9±0.0 | ND |
| 299-309(1330) | 10 | 4.5±0.0 | 4.9±0.1 | 4.0±0.1 | 4.3±0.4 |
| 310-321(1338) | 11 | 3.6±0.0 | 3.6±0.1 | 2.3±0.1 | 2.3±0.3 |
| 355-363(1175) | 7 | 4.2±0.1 | 5.6±0.1 | 5.2±0.2 | 3.7±0.2 |
| 363-374(1523) | 11 | 10.9±0.2 | 12.2±0.2 | 9.2±0.2 | 6.9±0.2 |
| 365-374(1297) | 9 | 8.9±0.1 | 9.3±0.1 | 8.0±0.2 | 6.9±0.1 |
| Phosphate binding cassette | | | | | |
| 337-353(1953) | 13 | 4.5±0.5 | 4.4 | 2.9±0.1 | 1.2 |
| 346-353(1175) | 5 | 1.2±0.3 | 1.2±0.3 | 0.9 | 0.8±0.1 |

* No. of deuterons exchanged over a 10 min time course obtained from kinetic plots of deuterons which fits best to a single exponential model. This models approximates the rates of fast changing deuterons (mainly solvent accessible amides) to a single rate.

# 4. Discussion

cAMP-dependent protein kinase and its mechanism of activation has been an object of study for more than two decades. Crystallographic studies complemented with Hydrogen/Deuterium exchange, mutagenesis and florescence anisotropy are some of the many techniques employed in the course of this understanding. Despite the extensive study of the individual subunits as well as the holoenzyme, the exact mechanism of activation has remained elusive. One of the keys to this mechanism would be in obtaining additional information about the intermediate state in the activation of PKA from the inactive holoenzyme state to the dissociated catalytic subunit.

The regulatory subunit is believed to exist in two stable conformations *in vivo* : the cAMP-free, PKA-C bound holoenzyme conformation and the cAMP saturated, PKA-C free conformation. Upon binding of cAMP the enzyme is activated and the R-subunit changes from the former conformation to the latter. This change occurs through an intermediate transient complex which consists of the holoenzyme bound to cAMP prior to dissociation. This state is relatively unstable, as the $K_D$ of the complex in the presence of cAMP is 0.2μM compared to 0.2nM in the absence of the ligand (20),(34). The relative concentrations of cAMP and PKA-C cause the ternary complex to toggle between each of the above mentioned stable conformational states (35). However, if trapped, the study of this ternary complex can provide some clues about the intrasubunit conformational changes that drive the activation of the enzyme.

The crystal structure of the PKA holoenzyme reveals detailed insights into intersubunit interactions in the PKA holoenzyme (27). The segments of RIα that directly interact with the C subunit include residues in the pseudosubstrate sequence (Arg94, Arg95, Ala97, Ile98 and Ser99), the linker region (Ala100,

Val102, Val103, and Glu105), the αXn-αA loop (Val134, Leu135, and His138), αA (Glu143), αB (Glu200, Leu201, Leu204 and Tyr205), and αC (Arg230, Leu233, Met234, Thr237, and Leu238)(27).

Complementary interface contributing regions in the C-subunit have been subdivided into 3 sites (site 1 mainly includes the glycine-rich loop, α:F and peptide positioning loop (residues Thr51 and Ser53, Gln84, Glu170, Gly200, Pro204 and Glu230)), (site 2 mainly includes the APE linker and a:G helix) (Ile210, Leu211, Lys213 Glu248, Val251)), (site 3 primarily includes the activation loop residues Arg 194, Thr195, Trp 196 and Thr 197)). Site 1 of the C-subunit thereby interacts with the inhibitor site of RIα, site 2 interacts on the C-subunit interacts with the αXn-αA loop, α:A, α:B and α:C of RIα.

cAMP which triggers the activation of the enzyme binds to a highly conserved V-shaped phosphate binding pocket (11) and its interactions at multiple sites send forth signals which have been mapped by several crystallographic and mutagenesis studies (23, 24, 11). A primary point of contact between cAMP and the PBC in the CBD-A is Arg209. The exocyclic equatorial oxygen of the cAMP phosphate interacts with Arg209, which further contacts the carboxylate of Asp170,present at the amino terminus of the β3 sheet. This Asp residue further relays the signal to Arg226 at the N-terminal of α-C sheet facilitating the dissociation of the RC holoenzyme.

Rp-cAMPS, a cAMP antagonist, with a sulfur substitution at the equatorial oxygen, binds the PBC and uncouples this charge relay because of the reduced electronegative polarity and steric hindrance. The Rp-cAMPS analog blocks the hypothesized signal relay originating from the equatorial oxygen-Arg209 interaction. This allows us to selectively view the effects of the Glu200 mediated

interaction. While the Sp-cAMPS analog maintains both points of interaction and hence acts as a close cAMP mimic as studied by the RIα(91-244):C.

Both the full length RC holoenzyme as well as the RIα(91-244):C complex were studied in the apo and Rp-cAMPS bound form. The exchange data allowed a comparison of the four complexes with each other and with the individual subunits. The RIα(91-244):C complex showed increased exchange in most of the regions in PKA-C as well as RIα(91-244) apart from the PBC, which showed decreased solvent accessibility corresponding to a difference of 1 deuteron exchanged, owing to the occupancy of the site by Rp-cAMPS.

**4.1 Effects of Rp-cAMPS binding can be traced to C-helix peptides in the R-C interface and when compared with the FL-RC complex shows interesting differences in solvent accessibilty.**

The 238-244 region in the α-C helix showed increased deuteration upon binding of Rp-cAMPS to the RIα(91-244):C complex. The RIα(91-244) is truncated at the end of the C-helix, the higher solvent exposure in the C-helix of RIα(91-244):C as compared to the FL complex is expected. However it is interesting to observe that the FL complex shows more solvent exposure in the C-helix compared to RIα(91-244):C when bound to Rp-cAMPS. Five residues of the C-helix participates in the R-C interface, - Arg230, Leu233, Met234, Thr237 and Leu238 (27). This change leads us to believe that the C-terminal end of this interaction site is almost completely disrupted.

A closer look of the C-helix of the RIα91-244:C complex reveals two overlapping peptides, m/z=994, residues 238-244 and m/z=881, residues 239-244 show an increase in deuteration by one deuteron in the former peptide (Fig. 4-1). As pepsin digestion cleaves the N-terminal amine of each peptide , the

exchange incurred by the peptide is representative of the segment beginning from N-terminal+1 residue (36).

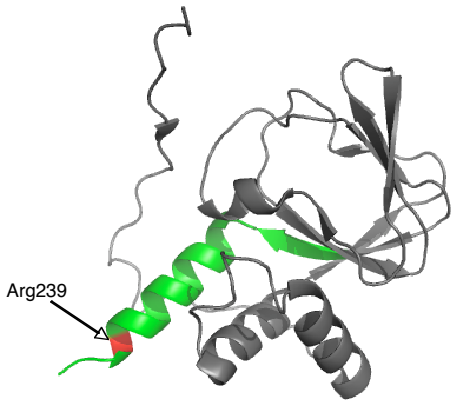


Figure 4-1. The RIα(91-244) subunit from the RIα(91-244):C complex was drawn using Pymol with the pdb file (accession number- 1u7e) (27). The C-helix (green) in RIα (91-244):C shows no change in deuteration upon Rp-cAMPS except the environment of Arg239 (red). The rest of the protein is labeled in grey.

Hence by subtractive analysis this change can be localized to the Arg239 residue. Amide exchange at the backbone amide reports on the environment of the residue, hence the change reported by Arg239 could reflect changes in the environment of Leu238 or Lys240. The Leu238 residue interacts with the C-subunit via van der Waals inteactions. This Leu238 residue is covered by the peptide m/z=1046, residues 230-238 which shows a significant reduction in exposure upon binding the C-subunit and retains almost the same accessibility when the complex binds Rp-cAMPS. This shows that the RC interface is stable in this region.

### 4.2 α-Xn helix and A-helix

The α-Xn helix interacts with the PKA-C subunit through Val134, Leu135 and His138 while the α:A helix has a single contact residue, Glu143. The corresponding interaction region at the C-subunit has been termed Site-2. The A-helix peptide m/z=1619, residues 136-143 shows no significant changes in the RIα(91-244):C complex when bound to Rp-cAMPS (Fig 4-2) while the α-Xn helix peptides m/z= 1619, residues 122-136 and m/z= 1783, residues 111-125 showed increased exchange upon binding Rp-cAMPS (Fig.4-2).

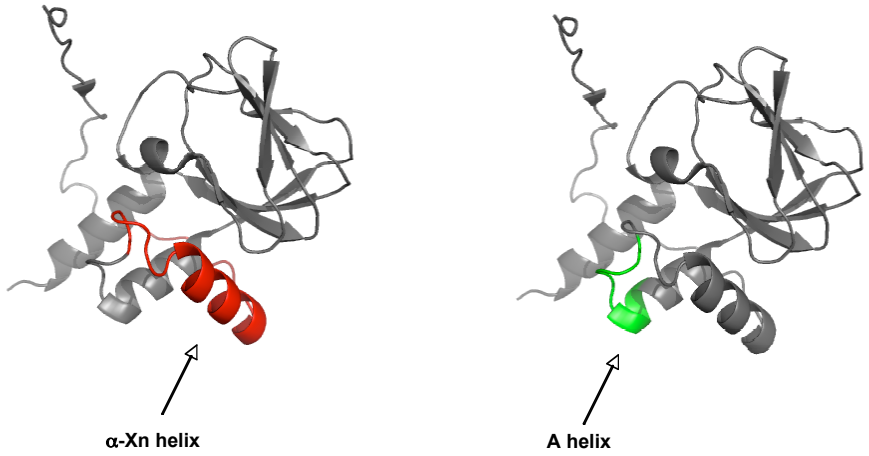


Figure 4-2. The RIα(91-244) subunit from the RIα(91-244):C complex was drawn using Pymol with the pdb file (accession number- 1u7e) (27). The α-Xn helix in RIα(91-244):C shows increased deuteration (red) while the A-helix shows no change in deuteration (green) upon binding Rp-cAMPS. The rest of the protein is labeled in grey.

The residues 111-125 in the α-Xn helix shows differences in solvent exposure in different states. The peptide shows no change when the RIα (91-244) subunit binds to Rp-cAMPS, however it becomes less exposed by almost three deuterons in the RIα(91-244):C complex. When Rp-cAMPS binds to the complex, this peptide becomes more exposed by nearly two deuterons(Table 1).This as well as the C-helix peptides convey that although some of the regions showing changes in exposure are not a part of the direct interface but the

changes they undergo influence the overall stability of the RIα(91-244):C complex. The data suggests that although the Rp-cAMPS analog locks the complex by binding to the phosphate binding cassette, it confers increased dynamics to the entire protein.

This provides the protein more degrees of freedom and hence more possible points of interaction when compared to a more stable structure. This entropic favorability coupled with the uncoupling of the charge relay responsible for dissociation of C-subunit may lead to the stability of this ternary complex. It has also been previously shown that Rp-cAMPS increases the rate of re-association of the RC complex by locking it in a favorable conformation. This study validates as well as localizes the changes in this ternary complex with respect to the apo form.

The changes noticed in the α-Xn helix and the single residue, Arg239 in the C-helix brought about by binding of Rp-cAMPS to the RIα(91-244):C are contributed solely by the signal transmitted by the 2'OH-Glu200 interaction. These changes could be correlated with increased solvent exposure in most of the C-lobe of PKA-C which contributes all of the sites of interaction with the regulatory subunit (Fig.4-3). This helped us localize the effects of this signal relay in PKA-C dissociation on PKA-C.

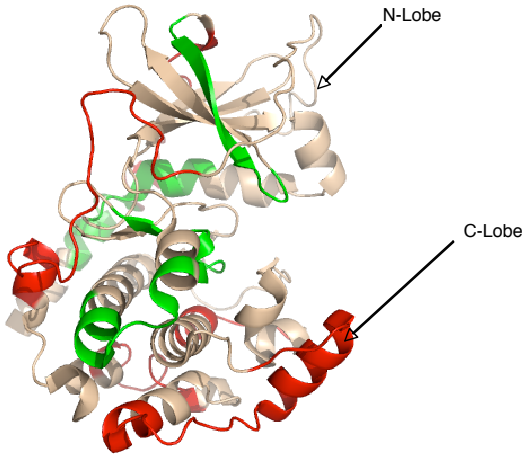


Figure 4-3. The RIα(91-244) subunit from the RIα(91-244):C complex was drawn using Pymol with the pdb file (accession number- 1u7e) (27). Increased solvent exposure(red) in most of the C-lobe of PKA-C in RIα(91-244):C. The regions labeled green showed no change in deuteration and the rest of the protein is labeled in sand color.

### 4.3 The effects of Sp-cAMPS binding on the RIα91-244:C reveals a different conformation than the Rp-cAMPS bound complex.

The binding of Sp-cAMPS to the RIα(91-244):C complex leads to increased exchange in the A-helix and as this region constitutes a part of the RC interaction interface, it points at a disruption of the interaction at this site (Fig. 4-4).

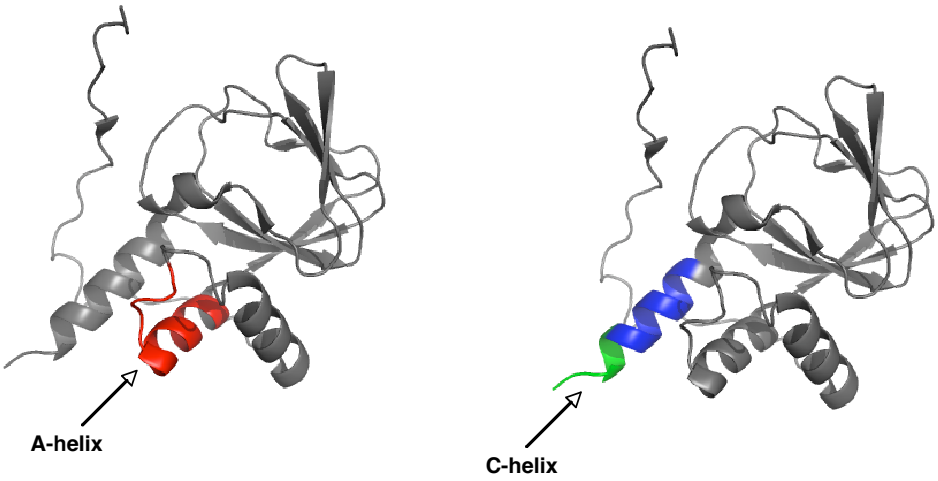


Figure 4-4. The A-helix shows increased exposure(red) while a major part of the C-helix shows decreased exposure(blue) in Sp-cAMPS bound ternary complex. The rest of the protein is labeled grey.

The C-helix showed protection upon binding Sp-cAMPS while the C-terminal end of the same helix showed no change (Fig.4-4). This change contrasts with the Rp-cAMPS bound complex where the same helix remains unchanged. The solvent protection might be due to the combined effects of excess PKA-C in the mixture and the binding of a cAMP like molecule. The Sp analog allows both the hypothesized signal relays to remain turned on which brings about a solvent exposure profile quite different from the RIα(91-244):C holoenzyme and the Rp-cAMPS bound ternary complex.

# 5. Conclusions

The effects of Rp-cAMPS binding when observed in the whole RIα (91-244):C complex (Fig.5-1) reveals increased dynamics in the ternary complex, substantiating the importance of the 2'OH-Glu200 interaction as playing a part in the dissociation of the complex. The primary site of interaction between PKA-C and RIα(91-244) is the active cleft- pseudosubstrate sequence interaction which is expected to remain intact as the Arg209 mediated signal that disturbs it is absent in the Rp-bound ternary complex. This coupled with increased entropy within the complex which also allows more degrees of freedom and consequently more possible points of interaction between the two interacting proteins, explains why the complex remains locked.

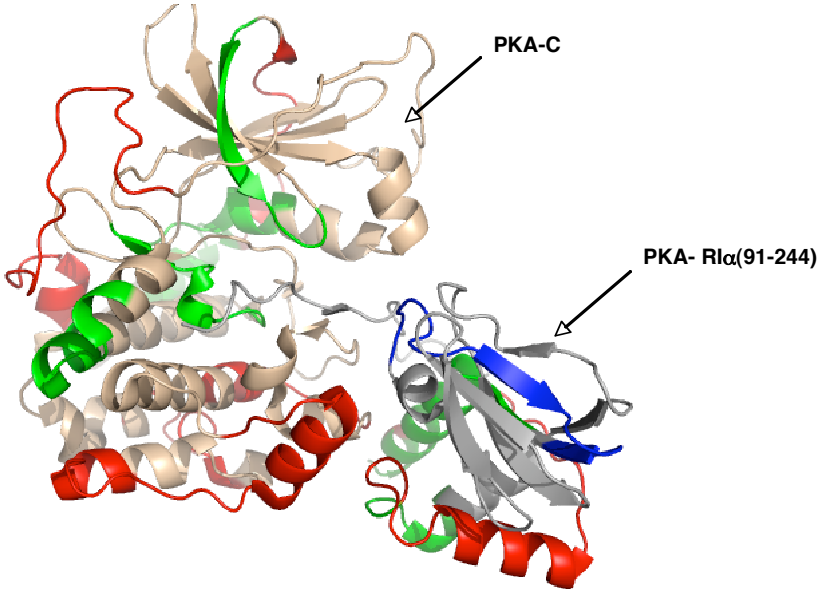


Figure 5-1. The RIα(91-244):C complex was drawn using Pymol with the pdb file (accession number- 1u7e) (27) displaying summary of H/$^{2}$H Exchange Data for the Ternary Complex, RIα91-244:C bound to Rp-cAMPS. The regions labeled in red showed increased exchange, the regions labeled in blue showed reduced exchange and the rest of the RIα91-244 protein was labeled grey and PKA-C was labeled sand.

The critical importance of the Arg209 mediated relay has been demonstrated by mutation studies previously (37) while the Glu200 has been known to be important for the binding of cAMP to the PBC. Our results show that the role of this interaction (2'OH-Glu200) extends beyond binding and partially contributes towards the dissociation of PKA-C from the RIα(91-244):C complex.

## References


1. Shabb, J. B., (2001) Physiological substrates of cAMP-dependent protein kinase. *Chem. Rev. 101*, 2381-24112.

2. Beebe, S. J., and Corbin, J. D., (1986). Cyclic nuclucleotide–dependent protein kinases. *The Enzymes 17*, 43-111.

3. Mitra, S., Zubay, G., and Landy, A. (1975). Evidence for the preferential binding of the catabolite gene activator protein (CAP)to DNA containing the *lac* promoter. *Biochem. Biophys. Res.Commun. 67*, 857-863.

4. Walsh, D. A., Perkins, J. P., and Krebs, E. G. (1968) An adenosine 3',5'-monophosphate-dependent protein kinase from rabbit skeletal muscle. *J. Biol. Chem*. *243*, 3763-3765.

5. Taylor, S. S., Buechler, J. A., and Yonemoto, W. (1990) cAMP dependent protein kinase: framework for a diverse family of regulatory enzymes. *Annu. Re*V*. Biochem*. *59*, 971-1005.

6. Ludwig, J., Margalit, T., Eismann, E., Lancet, D., and Kaupp, U.B. (1990) Primary structure of cAMP-gated channel from bovine olfactory epithelium. *FEBS Lett. 270*, 24-29.

7. de Rooij, J., Zwartkruis, F. J., Verheijen, M. H., Cool, R. H., Nijman, S. M., Wittinghofer, A., and Bos, J. L. (1998) Epac is a Rap1 guanine-nucleotide-exchange factor directly activated by cyclic AMP. *Nature 396*, 474-477.

8. Kawasaki, H., Springett, G. M., Mochizuki, N., Toki, S., Nakaya, M., Matsuda, M., Housman, D. E., and Graybiel, A. M. (1992) A family of

cAMP-binding proteins that directly activate Rap1. *Science 282*, 2275-2279.

9. Døskeland, S. O., Maronde, E., and Gjertsen, B. T. (1993) The genetic subtypes of cAMP-dependent protein kinase, Functionally different or redundant? *Biochim. Biophys. Acta 1178*, 249-258.

10. Scott, J. D. (1991) Cyclic nucleotide-dependent protein kinases. *Pharmacol. Ther. 50,* 123-145.

11. Leon, D.A., Canaves, J.M., and Taylor, S.S., (2000) Probing the multidomain structure of the type I regulatory subunit of cAMP-dependent protein kinase using mutational analysis: role and environment of endogenous tryptophans. *Biochemistry 39*, 5662-5671.

12. Ringheim, G. E., Saraswat, L. D., Bubis, J., and Taylor, S. S. (1988) Deletion of cAMP-binding site B in the regulatory subunit of cAMP-dependent protein kinase alters the photoaffinity labeling of site A. *J. Biol. Chem*. *263*, 18247-18252.

13. Neitzel, J. J., Dostmann, W. R. G., and Taylor, S. S. (1991) Role of MgATP in the activation and reassociation of cAMP-dependent protein kinase I: consequences of replacing the essential arginine in cAMP binding site A. *Biochemistry 30*, 733-739.

14. Herberg, F. W., Taylor, S. S., and Dostmann, W. R. G. (1996) Active site mutations define the pathway for the cooperative activation of cAMP-dependent protein kinase. *Biochemistry 35*, 2934-2942.

15. Øgreid, D., and Døskeland, S. O. (1981) The kinetics of association of cyclic AMP to the two types of binding sites associated with protein kinase II from bovine myocardium. *FEBS Lett 129,* 287-92.

16. Øgreid, D., and Døskeland, S. O. (1982) Activation of protein kinase isoenzymes under near physiological conditions. Evidence that both types (A and B) of cAMP binding sites are involved in the activation of protein kinase by cAMP and 8-N3-cAMP. *FEBS Lett 150*, 161-166.

17. Bubis, J., and Taylor, S. S. (1987) Correlation of photolabeling with occupancy of cAMP binding sites in the regulatory subunit of cAMP-dependent protein kinase I. *Biochemistry 26*, 3478-3486.

18. Øgreid, D. & Doskeland, S. O. (1983). Cyclic nucleotides modulate the release of [3H] adenosine cyclic 3',5'-phosphate bound to the regulatory moiety of protein kinase I by the catalytic subunit of the kinase. *Biochemistry 22*, 1686–1696.

19. Amieux, P.S., and McKnight, G.S. (2002) The essential role of RI alpha in the maintenance of regulated PKA activity. *Ann NY Acad Sci 968*, 75-95.

20. Anand, G.S., Taylor, S.S., and Johnson, D.A.(2007) Cyclic-AMP and Pseudosubstrate Effects on Type-I A-Kinase Regulatory and Catalytic Subunit Binding Kinetics. *Biochemistry 46,* 9283-9291.

21. Kopperud, R., Christensen, A. E., Kjarland, E., Viste, K., Kleivdal, H., and Doskeland, S. O. (2002) Formation of inactive cAMP saturated holoenzyme of cAMP-dependent protein kinase under physiological conditions, *J. Biol. Chem. 277*, 13443-13448.

22. Herberg, F. W., Dostmann, W. R. G., Zorn, M., Davis, S. J., and Taylor, S. S. (1994) Crosstalk between domains in the regulatory subunit of cAMP-dependent protein kinase : influence of amino terminus on cAMP binding and holoenzyme formation. *Biochemistry 33*, 7485–7494.

23. Huang,L.J.,and Taylor S.S.(1998)Dissecting cAMP Binding Domain A in the RIa Subunit of cAMP-dependent Protein Kinase. *J. Biol. Chem. 273*, 26739–26746.

24. Su,Y.,Dostmann, W. R. G., Herberg, F. W., Durick, K., Xuong, N-h., Ten Eyck, L., Taylor, S. S., Varughese, K.I. (1995) Regulatory Subunit of Protein Kinase A: Structure of Deletion Mutant with cAMP. *Science 269,* 807-813.

25. Canaves, J. M., and Taylor, S. S. (2002) Classification and phylogenetic analysis of the cAMP-dependent protein kinase regulatory subunit family. *J. Mol. Evol. 54*,17-29.

26. Anand, G. S., Hughes, C. A., Jones, J. M., Taylor, S. S. and Komives, E. A. (2002). Amide H/2H exchange reveals communication between the cAMP and catalytic subunit-binding sites in the R(I)alpha subunit of protein kinase A. *J. Mol. Biol. 323*, 377–386.

27. Kim, C., Xuong, N. H., and Taylor, S. S. (2005). Crystal structure of a complex between the catalytic and regulatory (RIalpha) subunits of PKA. *Science 307*, 690–696.

28. Ringheim, G. E., Saraswat, L. D., Bubis, J., and Taylor, S. S. (1988) Deletion of cAMP-binding site B in the regulatory subunit of cAMP-

dependent protein kinase alters the photoaffinity labeling of site A. *J. Biol. Chem. 263*, 18247-18252.

29. Dostmann, W. R. G., Taylor, S. S., Genieser, H. G., Jastorff, B., Døskeland, S. O., and Øgreid, D.(1990) Probing the cyclic nucleotide binding sites of cAMP-dependent protein kinases I and II with analogs of adenosine 3',5'-cyclic phosphorothioates. *J. Biol.Chem*. *265*, 10484-10491.

30. Wu, J., Jones, J.M., Xuong, N-h., Eyck, L.F.T., and Taylor. (2004) Crystal Structures of RIα Subunit of Cyclic Adenosine 5'-Monophosphate (cAMP)-Dependent Protein Kinase Complexed with (Rp)-Adenosine 3',5'-Cyclic Monophosphothioate and (Sp)-Adenosine 3',5'-Cyclic Monophosphothioate, the Phosphothioate Analogues of cAMP. *Biochemistry 43,* 6620-6629.

31. Mandell, J. G., Baerga-Ortiz, A., Akashi, S., Takio, K., and Komives, E. A. (2001) Solvent accessibility of the thrombin-thrombomodulin interface. *J. Mol.Biol. 306,* 575-589.

32. Mandell, J. G., Falick, A. M. and Komives, E. A. (1998) Measurement of amide hydrogen exchange by MALDI-TOF mass spectrometry. *Anal. Chem. 70,* 3987–3995.

33. Vigil, D., Lin, J.H., Sotriffer, C.A., Pennypacker, J.K., McCammon, J.A., and Taylor, S.S. (2006) A simple electrostatic switch important in the activation of type I protein kinase A by cyclic AMP. *Protein Sci. 15*, 113-21.

34. Kopperud, R., Christensen, A.E., Kjærland, E., Viste, K., Kleivdal, H.,and \ Døskeland, S.O. (2002) Formation of Inactive cAMP-saturated

Holoenzyme of cAMP dependent Protein Kinase under Physiological Conditions. *J. Biol. Chem*. *277,* 13443–13448.

35. Das, R., Esposito, V., Abu-Abed, M., Anand, G.S., Taylor, S.S., and Melacini G. (2007) cAMP activation of PKA defines an ancient signaling mechanism. *Proc. Natl. Acad. Sci. 104*, 93–98.

36. Bai, Y.W., Milne, J.S., Mayne, L. and Englander, S.W. (1993). Primary structure effects on peptide group hydrogen exchange. *Proteins: Struct. Funct. Genet. 17,* 75-86

37. Gibson, R.M., Ji-Buechler, Y., and Taylor, S.S. (1997) Identification of electrostatic interaction sites between the regulatory and catalytic subunits of cyclic AMP-dependent protein kinase. *Protein Sci. 6,* 25-34.